Effect of the Versatile Bifunctional Chelator AAZTA^5 on the Radiometal Labelling properties and the *in vitro* performance of a Gastrin Releasing Peptide Receptor Antagonist

Michael Hofstetter
Department of Nuclear Medicine, Inselspital, Bern, University Hospital
Euy Sung Moon
Department of Chemistry-TRIGA site, Johannes Gutenberg University Mainz
Fabio D'Angelo
Department of Nuclear Medicine, Inselspital, Bern, University Hospital
Lucien Geissbühler
Department of Nuclear Medicine, Inselspital, Bern, University Hospital
Ian Alberts
Department of Nuclear Medicine, Inselspital, University Hospital
Ali Afshar-Oromieh
Department of Nuclear Medicine, Inselspital, Bern, University Hospital
Frank Rösch
Department of Chemistry-TRIGA site, Johannes Gutenberg-University Mainz
Axel Rominger
Department of Nuclear Medicine, Inselspital, Bern, University Hospital
Eleni Gourni (eleni.gourni@insel.ch)
Department of Nuclear Medicine, Bern University Hospital https://orcid.org/0000-0003-2198-382X

Research article

Keywords: Gastrin Releasing Peptide receptor (GRPr), AAZTA, prostate cancer, imaging, peptide radionuclide therapy

Posted Date: August 18th, 2020

DOI: https://doi.org/10.21203/rs.3.rs-57438/v1

Version of Record: A version of this preprint was published at EJNMMI Radiopharmacy and Chemistry on November 30th, 2020. See the published version at https://doi.org/10.1186/s41181-020-00115-8.

Abstract

Background: Gastrin Releasing Peptide receptor (GRPr)-based radioligands, mainly antagonists, have shown great promise for diagnostic imaging of GRPr-positive cancers, such as prostate and breast.

The present study aims at developing and evaluating a versatile GRPr-based probe for both PET / SPECT imaging as well as intraoperative and therapeutic applications. The influence of the versatile chelator AAZTA^5 on the radiometal labelling properties and the *in vitro* performance of the generated radiotracers were thoroughly investigated.

The GRPr-based antagonist D-Phe-Gln-Trp-Ala-Val-Gly-His-Sta-Leu-NH_2 was functionalized with the chelator 6-[Bis(carboxymethyl)amino]-1,4-bis(carboyxmethyl)-6-methyl-1,4-diazepane (AAZTA^5) through the spacer 4-amino-1-carboxymethyl-piperidine (Pip) to obtain AAZTA^5-Pip-D-Phe-Gln-Trp-Ala-Val-Gly-His-Sta-Leu-NH_2 (LF1). LF1 was radiolabelled with ^{68}Ga (PET), ^{111}In (SPECT, intraoperative applications) and ^{177}Lu (therapy, SPECT). *In vitro* evaluation included stability studies, determination of lipophilicity, protein-binding studies, determination of K_d and B_{max} as well as internalization studies using the epithelial human prostate cancer cell line PC3. *In vitro* monotherapy as well as combination therapy studies were further performed to assess its applicability as a theranostic compound.

Results: LF1 was labelled with ^{68}Ga, ^{111}In and ^{177}Lu within 5 min at room temperature (RT). The molar activities (A_m) were ranging between 50-60 MBq/nmol for ^{68}Ga-LF1, 10-20 MBq/nmol for ^{111}In-LF1 and ^{177}Lu-LF1. The radiotracers were found to be stable for a period of 4 h post labeling exhibiting a hydrophilic profile with an average of a $LogD_{octanol/PBS}$ of -3, while the bound activity to the human serum protein was approximately 10%. $^{68/nat}$Ga-LF1, $^{177/nat}$Lu-LF1 and $^{111/nat}$In-LF1 exhibited high affinity for the PC3 cells, with K_d values of 16.27±2.45 nM, 10.25±2.73 nM and 5.16±1.94 nM, respectively, and the required concentration of the radiotracers to saturate the receptors (B_{max}) was between 0.5 and 0.8 nM which corresponds to approximately 4 x 10^5 receptors per cell. Low specific internalization rate was found in cell culture, while the total specific cell surface bound uptake always exceeded the internalized activity. *In vitro* therapy studies showed that combination of ^{177}Lu-LF1 with rapamycin inhibit the growth of PC3 cells more efficiently compared to ^{177}Lu-LF1 alone.

Conclusion: Encouraged by these promising *in vitro* data, preclinical evaluation of the LF1 precursor are planned in tumour models *in vivo*.

Background

The need to diagnose, prevent, and treat cancer is greater than ever, since cancer-associated deaths are still a major cause of deaths. Early detection is essential for effective treatment of the disease, hence, many efforts have been made to identify cancer related targets and to further investigate their implication in cancer management (Kumar et al. 2006). The G protein-coupled receptors (GPCR) are of high

importance since they have been identified as valuable targets for the development of specific radiotracers for solid tumor imaging in the field of nuclear medicine. The fundamental component for the successful development of GPCR-based radioligands for *in vivo* tumor imaging is the GPCR overexpression on tumors in combination with their low expression and limited density in the surrounding healthy organs (Reubi 2003) with somatostatin receptor being the first to be defined for *in vivo* imaging (Gibril et al. 1996). The successful clinical translation of somatostatin receptor targeting was the driving force for the identification of additional GPCR with the potential to be used for peptide receptor targeted diagnostic and therapeutic applications (Reubi 2013). Gastrin Releasing Peptide receptor (GRPr) that is overexpressed on a variety on human tumors, represents another target with high interest in nuclear medicine (Yu et al. 2013).

A high number of GRPr-based radiotracers, both agonists and antagonists, mainly derived from the N-terminal truncated octapeptide bombesin (7–14) have shown promising results (Mansi et al. 2016). GRPr-based radioagonists were the first to be developed. Although extensive preclinical research has been reported, only few radiotracers have been clinically assessed, mainly because of their mitogenic properties and the side effects. The diagnostic accuracy of ^{68}Ga-BZH3 was investigated in patients with gastrointestinal stromal tumors and gliomas (Dimitrakopoulou-Strauss et al. 2007; Strauss et al. 2012). Clinical trials have also been performed with the GRPr agonist AMBA, labeled with ^{68}Ga and ^{177}Lu in patients with various cancers, to assess its applicability as diagnostic as well as therapeutic radiopharmaceutical (Baum et al. 2007; Bodei et al. 2007). Furthermore, the feasibility of ^{99m}Tc-RP527 was evaluated in patients with prostate and breast cancer (Van de Wiele et al. 2001).

The significant finding of the somatostatin radioantagonists being preferable to radioagonists for *in vivo* peptide receptor targeting (Ginj et al. 2006) stimulated the shift towards the development of GRPr antagonists too (Cescato et al. 2008). A plethora of radioantagonists have been evaluated preclinically and since 2013 several clinical trials have been performed using GRPr radioantagonists (RM2 (or BAY 86-7548), RM26, NODAGA-MJ9, SB3, NeoBOMB1, TE2AAR06, BAY 86-4367) labeled with ^{68}Ga, ^{18}F, ^{64}Cu, ^{177}Lu, with ^{68}Ga-RM2 being the most deliberated one (Kähkönen et al. 2013; Roivainen et al. 2013; Wieser et al. 2014; Sah et al. 2015; Maina et al. 2016; Nock et al. 2017; Gnesin et al. 2018; Minamimoto et al. 2018; Zhang et al. 2018; Fassbender et al. 2019; Touijer et al. 2019). Baratto et al. recently used ^{68}Ga-RM2 to map its physiological distribution in humans. Pancreas was the organ with the highest uptake, followed by mild to moderate uptake in the gastrointestinal tract while the radiotracer is eliminated through the urinary tract (Baratto et al. 2019). The above radioantagonists were evaluated in patients with newly diagnosed prostate cancer (PC) and at biochemical recurrence of prostate cancer (BCR PC). In summary, the studies outline that the radioantagonists can be safely administrated to patients. They showed high detection rate of primary PC and BCR PC, were able to detect more lesions compared to ^{18}F-fluoroethylcholine and ^{99m}Tc-MDP, apparent performance was improved when compared with the radioagonist ^{68}Ga-BBN and exhibited higher detection rates compared to MRI.

The first in human dosimetry study with ^{177}Lu-RM2 was recently published. The therapy was well tolerated without side effects. Pancreas was the dose-limiting organ, bone metastases had the highest uptake, followed by lymph nodes and soft tissue lesions (Kurth et al. 2019).

RM2, RM26 and SB3 labeled with ^{68}Ga have also been used in few pilot studies to evaluate their detection rate in patients with primary breast cancer (Maina et al. 2016; Stoykow et al. 2016; Zang et al. 2018). These studies suggest that GRPr expression is correlated with estrogen receptors (ER) positive tumors, paving thus the way to expand additional the use of GRPr antagonists as a therapeutic tool.

Herein, the antagonistic statine-based GRPr peptide H-D-Phe-Gln-Trp-Ala-Val-Gly-His-Sta-Leu-NH_2 was functionalized with the chelator 6-[Bis(carboxymethyl)amino]-1,4-bis(carboyxmethyl)-6-methyl-1,4-diazepane (AAZTA^5) via the spacer 4-amino-1-carboxymethyl-piperidine (Pip) to obtain AAZTA^5-Pip-D-Phe-Gln-Trp-Ala-Val-Gly-His-Sta-Leu-NH_2 (LF1) (Fig. 1). LF1 was radiolabelled with ^{68}Ga, ^{111}In and ^{177}Lu. One of our goals was to investigate the influence of the versatile bifunctional chelator AAZTA^5 on the GRPr-based antagonist with regard to its receptor binding affinity and the *in vitro* performance of the generated radiotracers. Furthermore, the assessment of its potential in serving as theranostic compound for GRPr-positive tumors is also reported. The potent GRPr based antagonist RM2 was used as the reference compound (Fig. 1).

Materials And Methods

Reagents and Instrumentation

All reagents and solvents were of the best grade available and were obtained from Sigma-Aldrich, Merck, Fluka, AlfaAesar, VWR, AcrosOrganics and Fisher Scientific and used without further purification. They were provided with a septum. All culture reagents were from Gibco BRL, Life Technologies (Grand Island, NY). N.c.a. $^{177}LuCl_3$ and $^{111}InCl_3$ were obtained from Isotope Technologies Garching GmbH (ITG) (Munich, Germany) and b.e.Imaging GmbH (Baden-Baden, Germany), respectively. The GalliaPharm® Ge-68/Ga-68 Generator was available from Eckert & Ziegler (Berlin, Germany).

Deuterated solvents for NMR spectra were commercially available by Deutero. Thin layer chromatography plates from Merck, silica gel 60 F254 coated aluminium plates, were used for the analysis. Silica gel 60 (core size 0.063 / 0.200 mm) from Macherey-Nagel was used for purification by column chromatography.

The purification of the peptide was performed by semipreparative RP-HPLC on a 120-5 C18 Nucleosil column (250 x 21 mm) applying a linear gradient of 15-90% solvent B in 25 min at a flow rate of 12 mL / min (solvent A, 0.1% TFA / H_2O; solvent B, 0.1%TFA / Acetonitrile).

The quality control of the peptides as well as the radiolabeled compounds was performed by analytical RP-HPLC from Knauer advanced scientific instrument equipped with a Knauer Smartline Manager 5000, a Smartline Pump 1000 and a Smartline UV Detector 2600. The RP-HPLC runs were performed on an

analytical 120-5 C18 Nucleosil column (250 x 4.5 mm) applying a linear gradient of 15-90% solvent B in 25 min at a flow rate of 1 mL / min. (solvent A, 0.1% TFA / H_2O; solvent B, 0.1% TFA / Acetonitrile). Ultraviolet detection was performed using a Knauer detector at 240 nm. For radioactivity measurement, a Na(TI) well-type scintillation Gina star was used. The radiotracer solutions were prepared by dilution with 0.9% NaCl.

The human prostate adenocarcinoma cell line PC3 was obtained from CLS Cell Lines Service GmbH, (Eppelheim, Germany). Cell culture media Dulbecco's Modified Eagle Medium (DMEM) with GlutaMax-I Supplement, F-12 Nutrient Mixture with GlutaMax-I Supplement, Dubecco's Phosphate Buffered Saline (DPBS), Fetal Bovine Serum (FBS), Trypsin-EDTA and antibiotic solution Penicillin-Streptomycin were from Gibco BRL, Life Technologies (Grand Island, NY) and purchased from ThermoFisher (Switzerland).

ESI-MS mass spectra were acquired on a Bruker Daltonics Esquire 3000 plus device.

The ^{1}H-, ^{13}C-NMR measurements were performed on a Bruker Avance III HD 400 (400 MHz) or Avance III 600 (600 MHz). LC / MS spectra were measured on an Agilent Technologies 1220 Infinity LC system coupled to an Agilent Technologies 6130B Single Quadrupole LC / MS system.

TLC scans were acquired on an Elysia Raytest TLC scanner using the Gina Star TLC software.

Quantitative γ-counting was performed with a Cobra II Gamma Counter from Packard Instrument (USA).

All experiments were carried out twice in triplicates.

Synthesis of the prochelator AAZTA^{5}-(^{t}Bu)$_4$

The precursor AAZTA^{5}-(^{t}Bu)$_4$ was successfully synthesized over 4-steps following the protocol described by Sinnes et al. (Sinnes et al. 2019b). Briefly, the synthesis steps are described below and shown in Figure 2:

1,4-Dibenzyl-6-methylpentanoate-6-nitroperhydro-1,4-diazepane (**1**)

2-nitrocyclohexanone (2.00 g; 13.9 mmol) and Amberlyst A21 (1.05 g) were mixed with dry methanol (35 mL). The solution was heated to 60 °C and stirred under reflux for 1 h. *N,N'*-dibenzylethylene-diamine (3.36 g; 13.9 mmol) and paraformaldehyde (1.67 g; 55.5 mmol) were added to the solution. The suspension was heated to 80°C and stirred overnight. After completion of the reaction, the suspension was filtered and the filtrate concentrated under vacuum. After column chromatographic purification (CH / EA; 9:1; Rf= 0.27) a yellow oil was obtained as product **1** (5.20 g; 11.8 mmol; 85%).

1,4-Di(tert-butylacetate)-6-methylpentanoate-6-amino-di(tert-butylacetate)-perhydro-1,4-diazepine (**3**)

1 (1.05 g, 2.39 mmol) was added to a solution containing $Pd(OH)_2$ / C (0.62 g, 10 wt%) and abs. ethanol (20 mL). Acetic acid (411 µL; 7.18 mmol) was added, the solution was saturated with hydrogen and

stirred overnight at room temperature. After completion of the reaction, $Pd(OH)_2$ / C was filtered over Celite and the filtrate was concentrated under vacuum. Crude product **2**, a white-yellowish solid, was used for further reaction without further purification.

2 (1.05 g; 2.39 mmol) and K_2CO_3 (1.32 g; 9.57 mmol) were dissolved in dry acetonitrile (30 mL). *tert*-butyl bromoacetate (1.41 mL; 9.57 mmol) and potassium iodide (0.80 g) were added and stirred overnight at 40 °C. The solution was concentrated under vacuum and purified by column chromatography (CH / EA, 7:1; R_f= 0.15). Compound **3** was obtained as yellow oil (0.89 g; 1.30 mmol; 54%).

N,N'1,4-Di(tert-butylacetate)-6-pentanoicacid-6-(amino-di(tert-butylacetate))-perhydro-1,4-diazepine (**4**)

3 (293 mg, 0.43 mmol) was dissolved in 1,4-dioxane / water (2:1; 6 mL). 1 M LiOH solution (641 µL; 0.64 mmol) was added and stirred overnight at room temperature. After completion of the reaction, the solution was concentrated, the residue concentrated with 1 M $NaHCO_3$ solution and extracted several times with chloroform. The organic phase was extracted with water, dried with Mg_2SO_4 and concentrated under vacuum. Compound **4** was obtained a yellowish oil (224 mg; 0.33 mmol; 76%).

Synthesis of the Chelator-Peptide Conjugate

The peptide-chelator conjugate was synthesized manually using standard Fmoc chemistry and Rink amide 4-methylbenzhydrylamine resin. The spacer (Pip) and the prochelator ($AAZTA^5$-(^{t}Bu)$_4$) were consecutively coupled to the peptide using 1-[Bis(dimethylamino)methylene]-1H-1,2,3-triazolo[4,5-b]pyridinium 3-oxid hexafluorophosphate (HATU) as an activating agent. The cleavage of the peptide and the simultaneous deprotection of the side chain-protecting groups was performed using trifluoroacetic acid / triisopropylsilane / H_2O (95 / 2.5 / 2.5). The crude conjugate was further purified by semipreparative RP-HPLC as described in the “Reagents and Instrumentation” section.

Radiochemistry

^{68}Ga-LF1: The ^{68}Ga-labeled radiotracer was prepared within 5 min, using the Modular-Lab PharmTracer module by Eckert & Ziegler (Berlin, Germany). The radiolabeling performance of LF1 was assessed at pH 4.0 (0.2 M sodium acetate buffer), at RT using a conjugate amount of 5 - 20 µg (approximately 3 - 12 nmol). Briefly, the ^{68}Ge / ^{68}Ga-generator was eluted with 5 mL HCl 0.1 N and the eluate (~ 400 MBq) was loaded onto a cation exchange column (Strata-XC, Phenomenex). ^{68}Ga was eluted with 700 µL of a mixture of 5.5 M NaCl / 0.1 M HCl directly in a vial containing 400 µL of 1.8 M sodium acetate buffer, 2 mL H_2O, 200 µL of EtOH, 5 mg ascorbic acid / 20 µL H_2O and the tested amount of the conjugate, followed by SepPak C-18 purification to remove uncomplexed radiometal.

^{177}Lu-LF1 / ^{111}In-LF1 and ^{177}Lu-RM2: The ^{177}Lu- and ^{111}In-labeled radiotracers were prepared by dissolving 5-10 µg (approximately 3 - 6 nmol) of LF1 in 250 µL ammonium acetate buffer (0.5 M, pH 5.4),

followed by incubation with $^{177}LuCl_3$ (30 - 100 MBq) or $^{111}InCl_3$ (approximately 35 - 40 MBq) for 10 min at RT and were used without any further purification step.

After the labeling with ^{68}Ga, ^{177}Lu or ^{111}In and the quality control of the generated radiotracers, one equivalent of either $^{nat}Ga(NO_3)_3$ or $^{nat}LuCl_3$ x $6H_2O$ or $^{nat}InCl_3$ x $2H_2O$ were added to the relevant radiolabelling solutions. The final solutions were incubated at RT for 10 min to obtain structurally characterized homogeneous ligands which were used for the saturation binding studies.

Quality control of the radiotracers / Stability

Chemical and radiochemical purity of the tested solutions were determined using an analytical Nucleosil 100-5 C18 column applying the conditions described in the “Reagents and Instrumentation” section.

The presence of free $^{68}Ga^{3+}$ and $^{68}Ga^{3+}$-colloid in the ^{68}Ga-LF1 preparation was quantified by radio thin layer chromatography (Radio-TLC) using Silica gel 60-plates and two different mobile phase systems: a) 0.1 M Na-citrate; b) methanol / 1 M ammonium acetate (1 / 1, v / v). Using the first Radio-TLC system, the radiopeptide product and ^{68}Ga-colloid remain immobilized at the starting point, whereas free $^{68}Ga^{3+}$ ions move with the mobile phase. When the second system is used, only the labelled peptide moves with the mobile phase / solvent front.

The stability of the newly prepared radiotracers was tested via RP-HPLC for a period of 4 h post labeling.

Lipophilicity

The lipophilicity ($LogD_{octanol/PBS}$, pH 7.4) was estimated by the “shake-flask” method: The labeled conjugates (100 pmol; 1.08 MBq, 1.16 MBq and 0.50 MBq for ^{68}Ga-LF1, ^{177}Lu-LF1 and ^{111}In-LF1 respectively) were added to a solution of 1-octanol (500 µL) and of PBS (500 µL, pH 7.4). The mixture was vortexed for 1 h to reach the equilibrium and then centrifuged (3000 rpm) for 10 min. From each phase, an aliquot (50 to 100 µL) was pipetted out and measured in a gamma-counter. Each measurement was repeated five times. Care was taken to avoid cross-contamination between the phases. The partition coefficient was calculated as the average log ratio of the radioactivity in the organic fraction and the PBS fraction.

Protein binding studies in human plasma

^{68}Ga-LF1, ^{177}Lu-LF1 and ^{111}In-LF1 (100 pmol; 1.08 MBq, 1.16 MBq and 0.50 MBq for ^{68}Ga-LF1, ^{177}Lu-LF1 and ^{111}In-LF1 respectively) were incubated with human plasma (0.5 mL) at 37 °C for 30 min and 60 min respectively. When the incubating period was completed, proteins were precipitated with a solution of 1 mL of MeOH / ACN (1:1). Centrifugation (10 min, 9660g) for the separation of proteins was then performed. After careful separation of the two phases, the respective activities were measured in a gamma-counter, followed by determination of the percentage of each radiotracer which does not bind to the plasma proteins.

Cell culture

The human prostate epithelial adenocarcinoma cell line PC3, which is known to overexpress GRPr, was cultured at 37 °C and 5% CO_2 in Dulbecco's Modified Eagle Medium (DMEM) with GlutaMAX-I supplement and F-12 Nutrient Mix with GlutaMAX-I supplement in a ratio of 1:1. The medium was supplemented with 10% fetal bovine serum (FBS), penicillin (100 U / mL) and streptomycin (100 µg / mL).

Saturation Binding Studies

For receptor saturation analysis, PC3 cells were seeded at a density of 0.8 - 1 million cells per well in 6-well plates and incubated overnight with medium (DMEM : F12 (1:1) containing 1% FBS, 100 U/mL penicillin and 100 µg/mL streptomycin). The next day, the medium was removed, the cells washed and incubated for 1 h at 37 °C with fresh medium. Afterwards, the plates were placed on ice for 30 min followed by incubation with increasing concentrations of either $^{68/nat}$Ga-LF1 or $^{177/nat}$Lu-LF1 or $^{111/nat}$In-LF1 or $^{177/nat}$Lu-RM2 (1-100 nM) in phosphate-buffered saline binding buffer pH 7.4. After the addition of the radioligands, the cells were incubated for 120 min at 4 °C. Non-specific binding was determined in the presence of Tyr^4-Bombesin at a final concentration of 1 µM. Then the cells were washed twice with ice-cold PBS, followed by solubilization with 1 N NaOH and the cell-associated radioactivity was measured using a gamma-counter. Specific binding was plotted against the total molar concentration of the added radiotracer. The K_d values and the concentration of the radiotracer required to saturate the receptors (B_{max}) were determined by nonlinear regression using GraphPad (Prism 8 Graph Pad Software, San Diego, CA). For all the cell studies the values are normalized for 1x10^6 cells per well and all data are from two independent experiments with triplicates in each experiment.

Internalization Studies

For internalization experiments, PC3 cells were seeded into 6-well plates and treated as described above. Approximately 0.25 pmol of the respective radiopeptides were added to the medium and the cells were incubated (in triplicates) for 0.5, 1, 2, 4 and 6 h at 37 °C, 5% CO_2 for ^{177}Lu-LF1 and ^{111}In-LF1 and for 15, 30, 60, 90, 120, 180 and 240 min at 37 °C, 5% CO_2 for ^{68}Ga-LF1. To determine nonspecific membrane binding and internalization, excess of Tyr^4-Bombesin (final concentration 1 µM) was added to selected wells. At each time point, the internalization was stopped by removing the medium and washing the cells twice with ice-cold PBS. To remove the receptor-bound radioligand, an acid wash was carried out twice with a 0.1 M glycine buffer pH 2.8 for 5 min on ice. Finally, cells were solubilized with 1 N NaOH. The radioactivity of the culture medium, the receptor-bound, and the internalized fractions were measured in a γ-counter.

In vitro therapy studies with ^{177}Lu-LF1 in the presence or without rapamycin

For the *in vitro* therapy studies, PC3 cells were seeded at a density of 50000-100000 cells (depending on the investigating time point: 100000, 75000 and 50000 cells for 24, 48, 72 h respectively) in 12-well plates

and incubated overnight with cultivation medium at 37 °C and 5% CO_2. The next day, the medium was removed, the cells washed, and culture medium containing either rapamycin (10 nM) or DMSO (control medium) was added. The plates were incubated at 37 °C and 5% CO_2 for a period of 6 h. Afterwards, the medium containing rapamycin or DMSO was removed and fresh medium was added in each well. Furthermore, 1.85 MBq of ^{177}Lu-LF1 was added to preselected wells. The monotherapy (either with rapamycin or ^{177}Lu-LF1 alone) and combination therapy study (^{177}Lu-LF1 in presence of rapamycin) were performed in parallel with untreated cells which served as reference. The viability of the cells was accessed by the trypan blue exclusion assay after incubation at 37 °C and 5% CO_2 for 24, 48 and 72 h. The experiment was performed twice in triplicate.

Statistical Analysis

All data are expressed as the mean of values ± standard deviation (mean ± SD). Prism 8 Software (GraphPad Software) was used to determine statistical significance at the 95% confidence level, with a P value of less than 0.05 being considered significant.

Results

Synthesis of the prochelator AAZTA^5-(^{t}Bu)$_4$

The synthesis route of AAZTA^5-(^{t}Bu)$_4$ is shown in Figure 2. First, ring opening of 2-nitrocyclohexanone was carried out *in situ.* A diazepane ring was formed by reaction with *N,N'*-dibenzyldiamine via a double nitro-Mannich reaction, **1**. Hydrogenolysis using $Pd(OH)_2$ / C and H_2 removed the benzyl protecting groups at the endocyclic amines and simultaneously reduced the nitro group to an amine, **2**. The unstable product was directly reacted with *tert*-butyl bromoacetate without further purification to form tetra alkylated compound, **3**. Deprotection of the methyl ester protecting groups were carried out by using 1 M lithium hydroxide solution and 1,4-dioxane / H_2O (ratio 2:1) to receive the bifunctional chelator AAZTA^5-(^{t}Bu)$_4$, **4**.

The analytic data of the intermediate products **1** and **3** as well as the prochelator **4** are presented below:

Product **1**:

MS (ESI$^+$): m/z (%): 440.3 (M+H$^+$); calculated for $C_{25}H_{33}N_3O_4$: 439.25

^{1}H-NMR ($CDCl_3$, 400 MHz, δ [ppm]): 7.29 (m, 10 H); 3.66 (s, 3 H); 3.67 (dd, J = 13.5 Hz, 4 H); 3.25 (dd, J = 14.0 Hz, 4 H); 2.63 (m, 4 H); 2.12 (m, 2 H); 1.59 (m, 2 H); 1.32 (m, 2 H); 0.78 (m, 2 H). ^{13}C-NMR ($CDCl_3$, 100 MHz, δ [ppm]): 173.6 (s); 139.1 (s); 129.1 (s); 128.3 (s); 127.3 (s); 94.8 (s); 64.9 (s); 61.8 (s); 58.9 (s); 51.5 (s); 36.5 (s); 33.6 (s); 24.6 (s); 22.6 (s).

Product **3**:

MS (ESI$^+$): m/z (%): 686.5 (M+H$^+$); 708.4 (M+Na$^+$); calculated for $C_{35}H_{63}N_3O_{10}$: 685.45

^{1}H-NMR ($CDCl_3$, 400 MHz, δ [ppm]): 3.65 (s, 4 H); 3.61 (s, 4 H); 3.22 (s, 3 H); 2.99 (d, J = 14.1 Hz, 2 H); 2.85-2.65 (m, 4 H); 2.63 (d, J = 14.1 Hz, 2 H); 2.31 (t, J = 7.4 Hz, 2 H); 1.62-1.52 (m, 4 H); 1.44 (s, 18 H); 1.43 (s, 18 H); 1.25 (m, 2 H). ^{13}C-NMR ($CDCl_3$, 100 MHz, δ [ppm]): 174.4 (s); 172.9 (s); 170.9 (s); 80.9 (s); 80.4 (s); 65.3 (s); 63.2 (s); 62.6 (s); 59.4 (s); 52.1 (s); 51.6 (s); 37.3 (s); 34.3 (s); 28.3 (s); 28.3 (s); 25.9 (s); 21.8 (s).

Product **4** (AAZTA^5-(^{t}Bu)$_4$):

MS (ESI$^+$): m/z (%): 672.4 (M+H$^+$); 694.5 (M+Na$^+$); calculated for $C_{34}H_{61}N_3O_{10}$: 671.44

^{1}H-NMR ($CDCl_3$, 400 MHz, δ [ppm]): 3.60 (s, 4 H); 3.23 (s, 4 H); 3.00-2.97 (d, J = 14.1 Hz, 2 H); 2.88-2.60 (m, 6 H); 2.36-2.32 (t, J = 7.9 Hz, 2 H); 1.64-1.52 (m, 4 H); 1.43 (s, 18 H); 1.42 (s, 18 H); 1.24 (m, 2 H). ^{13}C-NMR ($CDCl_3$, 100 MHz, δ [ppm]): 178.9 (s); 172.9 (s); 170.9 (s); 81.0 (s); 80.5 (s); 65.1 (s); 63.1 (s); 59.4 (s); 52.2 (s); 34.2 (s); 29.8 (s); 28.3 (s); 28.2 (s); 25.6 (s); 22.8 (s); 21.9.

Synthesis of the Chelator-Peptide Conjugate

The synthesis yields of the peptide-chelator conjugate ranged from 30 to 40 %. The purity and identity of the peptids was >95% as determined by HPLC and mass spectroscopy. The analytical data are depicted in Table 1.

A reception control (HPLC and mass spectroscopy) of the compound RM2 (GMP grade) was also performed at our department and the analytical data are reported in Table 1.

Table 1. Analytical data of LF1 and RM2.

Compound	Elemental composition	Purity	Calculated mass	MS (ESI)	Rt (min)
LF1	$C_{80}H_{116}N_{18}O_{22}$	>95%	1682.89 m/z [M+H$^+$]	1623.89 m/z	13.8
RM2	$C_{78}H_{118}N_{20}O_{19}$	>95%	1638.89 m/z [M$^{+\cdot}$]	1638.89 m/z	12.8

Radiochemistry / Quality control / Stability

^{68}Ga-LF1:

LF1 (3, 6 and 12 nmol) was labeled with ^{68}Ga with a labeling yield of about 90%. HPLC revealed the formation of one additional radioactive species (about 10%). The retention time of the main peak was 12.8 min while the retention time of the second radioactive species was 12.1. TLC excluded the creation of gallium colloids. The maximum achieved molar activity (A_m) was approximately 60 MBq / nmol.

^{177}Lu-LF1 and ^{111}In-LF1: LF1 was labeled with ^{177}Lu and ^{111}In at RT with a labeling yield >98%. Both analytical methods, HLPC and TLC verified the presence of one radioactive species (the corresponding radiolabeled peptide in each case) while the percentage of the free metal was <2%. The retention times of ^{177}Lu-LF1 and ^{111}In-LF1 were 12.7 and 14.5 min respectively. The molar activities (A_m) were ranging 10 - 20 MBq / nmol for ^{177}Lu-LF1 and approximately 10 MBq / nmol for the ^{111}In-labeled radioligand.

The stability of all the radiotracers over time was determined with RP-HPLC and neither radiolysis or decomposition was observed for a period of 4 hour post labeling.

Lipophilicity / Protein binding studies in human plasma

With a $LogD_{octanol/PBS}$ of -3.17 ± 0.04, -2.89 ± 0.04 and -2.75 ± 0.08 for ^{68}Ga-LF1, ^{177}Lu-LF1 and ^{111}In-LF1, respectively, all the radiotracers show a hydrophilic profile. (Lipophilicity = the logarithm of the partition coefficient D, where D is the ratio of the distribution of a compound in 2 solvents, here octanol and PBS).

To estimate the bioavailability of ^{68}Ga-LF1, ^{177}Lu-LF1 and ^{111}In-LF1 in circulation, the extent of human plasma protein binding was determined. Approximately 10% of the incubating ^{68}Ga, ^{177}Lu and ^{111}In activity was found to be bound to plasma proteins at the tested time points.

Saturation Binding Studies

Saturation binding studies were performed at 4 °C, in order to allow binding of the radioconjugates to the receptor but to avoid endocytosis. All the radiotracers exhibited affinity for the GRPr positive PC3 cells, with K_d values of 16.27 ± 2.45 nM for $^{68/nat}$Ga-LF1, 10.25 ± 2.73 nM for $^{177/nat}$Lu-LF1 and 5.16 ± 1.94 nM for $^{111/nat}$In-LF1 (Figure 3). The B_{max} values were also at the same level for the three radiotracers (0.44 ± 0.02 nM for $^{68/nat}$Ga-LF1, 0.79 ± 0.05 nM for $^{177/nat}$Lu-LF1 and 0.59 ± 0.06 nM for $^{111/nat}$In-LF1) which correspond to approximately 4 x 10^5 receptors per cell.

The side-by-side comparison with the high affinity GRPr antagonist RM2 revealed that the affinities of the new tested radiotracers were at the same range with $^{177/nat}$Lu-RM2 (K_d: 5.42 ± 0.84 nM and B_{max}: 0.82 ± 0.03 nM).

Internalization Studies

^{68}Ga-LF1, ^{177}Lu-LF1 and ^{111}In-LF1 were found to be well associated with the PC3 cells within the incubation time frame (Figure 4). Continued exposure of the cells to the radioactive ligands resulted in a gradual increase of the total cell associated uptake from 15 min to 4 h for ^{68}Ga-LF1 and from 30 min to 6 h for ^{177}Lu-LF1 and ^{111}In-LF1. ^{111}In-LF1 exhibited the higher total cell associated uptake (38.3 ± 2.5 %) followed by ^{177}Lu-LF1 (34.5 ± 2.3 %) at 6 h (P=0.0035). ^{68}Ga-LF1 revealed the lowest cell associated uptake (13.1 ± 0.24 %). At 6 h, the amount of specifically internalized activity was 9.2 ± 0.5% for ^{111}In-LF1 and 8.9 ± 0.8% for ^{177}Lu-LF1 (P=0.0054), while ^{68}Ga-LF1 exhibited 2.8 ± 0.5% internalized activity at 4 h.

Blocking experiments performed with excess of Tyr^4-BN, showed negligible nonspecific binding on the cell surface, while less than 0.3% of total added radioactivity was found to be internalized (data not shown) demonstrating the high specificity of the GRPr-conjugates towards PC3 cells.

In vitro therapy studies with ^{177}Lu-LF1 in the presence or without rapamycin

An *in vitro* therapy study was performed aiming at evaluating the effect of combination therapy on PC3 cells (Figure 5). The viability of PC3 cells was verified 48 and 72 h after treatment. The chosen dose of rapamycin for the *in vitro* therapy studies was 10 nM, since it has been previously shown that rapamycin at this concentration has the greatest cytostatic effect on PC3 cells (Dumont et al. 2013). The applied dose of ^{177}Lu-LF1 was 1.85 MBq. Combination therapy was found to be slightly more effective compared to rapamycin or ^{177}Lu-LF1 alone (cell viability: approx. 40%, 48 and 72 h after the treatment). The treatment only with rapamycin showed a higher impact compared to ^{177}Lu-LF1 on PC3 cells (cell viability: approx. 50% for rapamycin and 70 % ^{177}Lu-LF1 72 h).

Discussion

Prostate cancer, a complex and biologically heterogeneous disease, is the most common type of cancer found in men, which often begins without symptoms. It is on a spectrum varying from asymptomatic and slow-growing disease to a more aggressive and rapidly progressive systemic malignancy (Kelloff et al. 2009). The survival rate could, therefore, be significantly improved when early detection and personalized treatment take place. Photon emission computed tomography (SPECT) and positron emission tomography (PET) have gained a lot of attention in the management of prostate cancer due to their high accuracy rate. Even though the results of most commonly used oncological radiotracers ^{18}F-FDG and ^{18}F-choline PET, in delineating primary prostate cancers, were confused (Hofer et al. 1999; Liu et al. 2001), several attempts have been made to improve the usefulness of SPECT and PET. The scientific attention has been, therefore, shifted towards the development and validation of molecular probes, which exhibit higher sensitivity and specificity compare to ^{18}F-FDG and ^{18}F-choline. The overexpression of peptide receptors on the surface of prostate cancer cells played a pivotal role in this development and consequently generated interest in the investigation of radiolabeled peptide-based probes for radio-theranostic applications. Prostate Specific Membrane Antigen (PSMA) and GRPr are the two receptors, which are overexpressed on the surface of prostate cancer cells rendering them promising targets for prostate cancer imaging and potential therapy. Many efforts have been made towards the development of PSMA- and GRPr-based imaging agents with a particular focus on the low molecular weight PSMA inhibitors and the GRPr-based antagonists. PSMA theranostics have proven great success in prostate cancer management in the recent years (Eder et al. 2012; Afshar-Oromieh et al. 2017). However, due to low PSMA expression not all patients suffering from prostate cancer can benefit from the advantages of PSMA targeting. Therefore, there is an urgent need for these patients for both characterization, planning, monitoring of the cancerous disease and treatment itself. Furthermore, because of the noticeable heterogeneity of prostate cancer at the time of diagnosis (Schrecengost and Knudsen 2013), and even

more during the recurrence (Scher et al. 2013), it might be possible that the combination of imaging probes would provide clinical advantages with respect to the imaging of various types and stages of prostate cancer. Amongst the GRPr-based antagonists which have been clinically translated (Baratto et al. 2020), RM2 is the one which has been used in most clinical studies. GRPr and PSMA expression were compared on primary prostate cancer samples (Schollhammer et al. 2019; Touijer et al. 2019) as well as patients (Baratto et al. 2020) providing evidence that the biodstribution for the two radioligands were distinct. These significant findings suggest that GRPr and PSMA expression may provide complementary information to fully characterize prostate cancer. The so far preliminary data shows that the low metastatic risk PC patients could benefit from GRPr targeting while in high-risk patients the PSMA-based radiotracers could serve as a valuable tool (Minamimoto et al. 2016).

Our goal was to develop and evaluate a versatile probe suitable for imaging of GRPr-positive tumors followed by therapeutic applications. Thus, the chelator AAZTA^5 was conjugated to the potent statine-based GRPr antagonist D-Phe-Gln-Trp-Ala-Val-Gly-His-Sta-Leu-NH_2, through the positively charged Pip linker, since previous findings support that the presence of a positively charged spacer improves the binding affinity of the derived GRPr-based ligand (Mansi et al. 2011; Gourni et al. 2014). A considerable amount of ongoing research developments is focused in the direction of bridging radiopharmaceuticals within a theranostic framework, the aim being to generate a single probe for both diagnosis and treatment. The selection of an appropriate chelator, which bears excellent coordination ability for diagnostic and therapeutic radionuclides, consists the key step of this approach. The most frequently used chelator for radiopharmaceuticals in clinical routine applications, DOTA (1,4,7,10-tetraazacyclododecane-1,4,7,10-tetraacetic acid), has shown great ability for binding a variety of radiometals such as ^{68}Ga, ^{111}In, ^{90}Y, ^{64}Cu, ^{177}Lu. However, its applicability presents some limitations since efficient radiolabeling yields are achieved between 80 and 100 °C and the optimum labeling pH is 3 to 5 (Price and Orvig 2014). Other macrocyclic-based chelators which have been extensively used mainly in preclinical developments is NOTA (1,4,7-triazacyclononane-1,4,7-triacetic acid) and its derivative NODAGA (1,4,7-triazacyclononane, 1-glutaric acid-4,7 acetic acid), which could enable sufficient labeling yields in lower temperatures compared to DOTA but in this case lower specific activities compared to the DOTA-coupled conjugates are reported. The biggest disadvantage of NOTA and NODAGA is that their cavity is not suitable for the incorporation of therapeutic radionuclides such as ^{177}Lu (Eisenwiener et al. 2002). The acyclic chelating agent, HBED-CC (*N,N*′-bis-[2-hydroxy-5-(carboxyethyl)benzyl]ethylenediamine-*N,N*′-diacetic acid) which has been used for the functionalization of the PSMA inhibitor PSMA-11, allows efficient radiolabelling with ^{68}Ga even at ambient temperature, but it forms multiple radiolabeled species when complexed to Ga^{3+} (Eder et al. 2014). Therefore, a bifunctional chelator which could surmount the above obstacles would be the optimum choice for the development of a new class of radiotracers. AAZTA^5, a versatile chelator could be considered as a potential candidate for this purpose. While AAZTA was initially developed for the chelation of Gd(III) as an MRI agent (Aime et al. 2004), it was shown that it exhibits high coordination capability for a variety of metal ions such as ^{68}Ga, ^{111}In, ^{177}Lu, ^{44}Sc (Eisenwiener et al. 2002; Waldron et al. 2013; Pfister et al. 2015; Tsionou et al. 2017; Sinnes et al. 2019a).

In particular, the mesocyclic structure of AAZTA^5 facilitates efficient labeling with high specific activities with a variety of radionuclides at RT and even at near neutral pH, optimal conditions for small proteins. Throughout this study, our main goal was to investigate whether and how N-terminal modulations, via the coupling with AAZTA^5, may influence the affinity of the derived GRPr-based radioligand towards GRPr, with a particular focus on additional *in vitro* studies that allow us to assess the suitability of these radiotracers for further evaluation. Furthermore, attention was given on the radiometal labeling properties of LF1 after its labeling with ^{68}Ga (PET), ^{177}Lu (therapy, SPECT) and ^{111}In (SPECT, intraoperative applications).

Radiolabeling with ^{177}Lu and ^{111}In was fast and quantitative at RT and pH 5.4 with precursor amounts between 3 and 6 nmol. These findings support the applicability of the AAZTA^5-coupled conjugates for sufficient labeling under mild conditions, even at nearly neutral pH. The stability of ^{177}Lu-LF1 and ^{111}In-LF1 over time was tested for a period of 4 h post labeling. No release of free radiometals was observed. Their high stability in combination with their hydrophilic character may have resulted in the low binding to the proteins of human serum (around 10%) as shown by our *in vitro* studies.

When the AAZTA^5-coupled GRPr conjugate was labeled with ^{68}Ga at pH 4.0 two radiolabeled species were observed by radio-HPLC while Waldron et al. reported the presence of three radioactive species when they labeled AAZTA with ^{68}Ga under the same conditions (Waldron et al. 2013). Since the difference of the retention time between the two observed species was less than 1 min we cannot fully exclude the formation of one additional species. The stability of the radiolabeled compound was assessed over a period of 3 h without observing any alterations on the HPLC profile. Modification at the iminodiacetate moiety where one of the acetate groups could be replaced by a methyl group may prevent the formation of side products.

The observed differences of ^{68}Ga-LF1 compared to ^{177}Lu-LF1 and ^{111}In-LF1 with regard to their radiochemical purity prompt us to further investigate if their GRPr binding affinity is influenced and to what extent. Additionally, a side-by-side comparison of their binding affinities along with the binding affinity of ^{177}Lu-RM2, which served as a reference peptide in this study, was also performed. ^{111}In-LF1 (K_d: 5.16 ± 1.94 nM) was the most affine exhibiting a Kd value similar to ^{177}Lu-RM2 (K_d: 5.42 ± 0.84 nM) followed by ^{177}Lu-LF1 (K_d: 10.25 ± 2.73 nM). ^{68}Ga-LF1 (K_d: 16.27 ± 2.45 nM) was still affine towards GRPr, however, the tracer with the lowest affinity amongst the three almost by a factor of 3 compared to ^{111}In-LF1. This finding led us to the conclusion that the minor radioactive species which was formed during the labeling of LF1 with ^{68}Ga may influence the affinity of the main formed product. Since for AAZTA, the N_2O_4 coordination may also occur in a competitive way with the favorable N_3O_3 coordination, this might be the reason of the decreased affinity of ^{68}Ga-LF1 compared to ^{177}Lu- and ^{111}In-LF1. These findings were further supported by the *in vitro* internalization studies, which demonstrated high and selective binding of ^{68}Ga-LF1, ^{177}Lu-LF1 and ^{111}In-LF1 to GRPr overexpressing cells. ^{177}Lu-LF1 and ^{111}In-LF1 exhibited a comparable profile in terms of total cell associated uptake (about 35% at 6 h) and

percentage of specific internalized fraction (about 10% at 6 h) while the corresponding values of ^{68}Ga-LF1 were approximately 14% and 3% respectively at 4 h. The radiolabeling as well as the *in vitro* performance may eliminate the applicability of ^{68}Ga-LF1 as a PET radiotracer. However, AAZTA may be a suitable chelator for other PET radionuclides, such as ^{44}Sc and ^{64}Cu and the potential of LF1 to serve as a PET tracer after its labeling with those radionuclides should also be evaluated. Furthermore, ^{44}Sc and ^{64}Cu due to their longer half-life (3.97 and 12.7 h, respectively) compared to ^{68}Ga (67.7 min) allow late imaging. This is of paramount importance especially in case of GRPr expression imaging, since preclinical (Gourni et al. 2014) as well as clinical data (Wieser et al. 2014) have shown that late imaging may be favorable due to the efficient background clearance compared to the tumor.

Our results from the comparative internalization studies between ^{68}Ga-LF1, ^{177}Lu-LF1 and ^{111}In-LF1, showed that the surface associated activity exceeded the amount of internalized activity at all-time points. In previous studies (Mansi et al. 2011), it was shown that RM2 at a concentration of 10 μM does not cause any effect on calcium mobilization after its incubation with PC3 cells, while an immunofluorescence assay revealed no receptor internalization of the DOTA-Pip-conjugate RM2. The previously confirmed antagonistic potency of RM2 in combination with our findings led us to the assumption that the introduction of AAZTA^5 did not change the antagonist features of the statine-based motif and that LF1 retains its GRPr-antagonistic profile.

In a next step, the assessment of the potential of LF1 in serving as theranostic compound for GRPr-positive tumors was investigated. Therefore, an *in vitro* therapy study was executed with the aim to evaluate the effect of combination therapy on PC3 cells after their treatment with rapamycin, a FDA approved specific inhibitor of mTOR. The phosphoinositide 3-kinase (PI3K) / protein kinase B (AKT) / mammalian target of rapamycin (mTOR) pathway regulates several physiological functions such as control of cell metabolism, growth, proliferation and survival. Studies have also shown that the (PI3K) / Akt / mTOR pathway is activated in several tumor cancers, in particular in 30%–50% of PC, mainly due to the amplification of gene encoding components, advocating that targeted inhibition of those individual components of the signaling cascade might be a solid strategy for cancer therapy (Gomez-Pinillos and Ferrari 2012). Furthermore, rapamycin has shown to inhibit tumor growth, angiogenesis, metastasis and cause apoptosis in cancer cell lines as well as in tumor mouse models (Konings et al. 2009). PC3 cells were used as the *in vitro* model since the (PI3K) / Akt / mTOR pathway is upregulated (Edlind and Hsieh 2014). Our preliminary *in vitro* data showed that combination therapy was slightly more effective compared to monotherapy with ^{177}Lu-LF1, suggesting that the mTOR kinase inhibition may contribute to the sensitization of the malignant prostate cancer cells to radiation, which would lead to amplification of tumor response and consequently lower therapeutic doses. This is of great importance in targeted radiotherapy since the lower irradiation results in minimizing the toxicity of the surrounding tissue and the limiting organ such as pancreas in case of GRPr targeting organs. *In vivo* studies are planned to be performed in order to define the ideal therapeutic doses and therapy regimens.

Conclusion

On the basis of the current results, LF1 labeled ^{177}Lu and ^{111}In appears to have a considerable potential to serve as a versatile probe suitable for SPECT, therapy and intraoperative applications. The ease of LF1 synthesis, the efficient radiolabeling at RT with a variety of radiometals, the stable encapsulation of ^{177}Lu and ^{111}In by AAZTA^5 and their favorable *in vitro* performance renders them suitable candidates for further extensive *in vivo* studies.

In vivo studies are planned to be performed which together with the already *in vitro* data may provide a solid evidence for their clinical translation.

Declarations

Ethics approval and consent to participate

Not applicable.

Consent for publication

All authors gave their consent for publication

Availability of data and materials

All data generated or analyzed during this study are included in this published article.

Competing interests / Funding

All authors declare that they have no competing interest associated with this publication and there has been no significant financial support.

Authors' contributions

All the authors read and approved the final manuscript.

EG, AR and FR have designed the study; MF, ESM, FA, LG performed the chemistry and radiochemistry experiments; MF, FA and LG performed the in vitro experiments; all authors analysed the data. EG and AR wrote and approved the final manuscript.

Acknowledgements

We thank Prof Dr Helmut R. Maecke and Prof. Dr. Philipp T. Meyer from the Department of Nuclear Medicine, University Hospital Freiburg, Germany, for kindly providing us the compound RM2.

Abbreviations

GPCR: G protein-coupled receptors

GRPr: Gastrin Releasing Peptide receptor

PC: prostate cancer

BCR PC: biochemical recurrence of prostate cancer

ER: estrogen receptors

AAZTA^5: 6-[Bis(carboxymethyl)amino]-1,4-bis(carboyxmethyl)-6-methyl-1,4-diazepane

DOTA: 1,4,7,10-tetraazacyclododecane-1,4,7,10-tetraacetic acid

NOTA: 1,4,7-triazacyclononane-1,4,7-triacetic acid

NODAGA: 1,4,7-triazacyclononane, 1-glutaric acid-4,7 acetic acid

HBED-CC: *N,N'*-bis-[2-hydroxy-5-(carboxyethyl)benzyl]ethylenediamine-*N,N'*-diacetic acid

Pip: 4-amino-1-carboxymethyl-piperidine

TFA: Trifluoroacetic acid

DPBS: Phosphate Buffered Saline

FBS: Fetal Bovine Serum

ESI-MS: electrospray ionization mass spectrometry

LC-MS: Liquidchromatography–mass spectrometry

TLC: Thin Layer Chromatography

HPLC: High-performance liquid chromatography

HATU: 1-[Bis(dimethylamino)methylene]-1H-1,2,3-triazolo[4,5-b]pyridinium 3-oxid hexafluorophosphate

HEPES: (4-(2-hydroxyethyl)-1-piperazineethanesulfonic acid)

ACN: Acetonitrile

A_m: Molar activities

RT: room temperature

MRI: Magnetic resonance imaging

SPECT: Photon emission computed tomography

PET: Positron emission tomography

PSMA: Prostate Specific Membrane Antigen

PI3K: phosphoinositide 3-kinase

AKT: protein kinase B

mTOR: mammalian target of rapamycin

References

1. Afshar-Oromieh A, Holland-Letz T, Giesel FL, Kratochwil C, Mier W, Haufe S, et al. Diagnostic performance of ^{68}Ga-PSMA-11 (HBED-CC) PET/CT in patients with recurrent prostate cancer: evaluation in 1007 patients. Eur J Nucl Med Mol Imaging. 2017 Aug;44(8):1258–68.
2. Aime S, Calabi L, Cavallotti C, Gianolio E, Giovenzana GB, Losi P, et al. [Gd-AAZTA]-: a new structural entry for an improved generation of MRI contrast agents. Inorg Chem. 2004 Nov 29;43(24):7588–90.
3. Baratto L, Duan H, Laudicella R, Toriihara A, Hatami N, Ferri V, et al. Physiological ^{68}Ga-RM2 uptake in patients with biochemically recurrent prostate cancer: an atlas of semi-quantitative measurements. Eur J Nucl Med Mol Imaging. 2019 Sep 2.
4. Baratto L, Duan H, Maecke HR, Iagaru A. Imaging the Distribution of Gastrin Releasing Peptide Receptors in Cancer. J Nucl Med. 2020 Feb 14.
5. Baum RP, Prasad V, Mutloka N. Molecular imaging of bombesin receptors in various tumors by Ga-68 AMBA PET/CT: First results. J Nucl Med. 2007;48:79P.
6. Bodei L, Ferrari M, Nunn A, Llull J, Cremonesi M, Martano L, et al. Lu-177-AMBA Bombesin Analogue in Hormone Refractory Prostate Cancer Patients: A Phase i Escalation Study with Single-Cycle Administrations. Eur J Nucl Med Mol Imaging. 2007;34:221–1.
7. Cescato R, Maina T, Nock B, Nikolopoulou A, Charalambidis D, Piccand V, et al. Bombesin receptor antagonists may be preferable to agonists for tumor targeting. J Nucl Med. 2008 Feb;49(2):318–26.
8. Dimitrakopoulou-Strauss A, Hohenberger P, Haberkorn U, Mäcke HR, Eisenhut M, Strauss LG. ^{68}Ga-labeled bombesin studies in patients with gastrointestinal stromal tumors: comparison with ^{18}F-FDG. J Nucl Med. 2007 Aug;48(8):1245–50.
9. Dumont RA, Tamma M, Braun F, Borkowski S, Reubi JC, Maecke H, et al. Targeted Radiotherapy of Prostate Cancer with a Gastrin-Releasing Peptide Receptor Antagonist Is Effective as Monotherapy and in Combination with Rapamycin. J Nucl Med. 2013 May 1;54(5):762–9.
10. Eder M, Neels O, Müller M, Bauder-Wüst U, Remde Y, Schäfer M, et al. Novel Preclinical and Radiopharmaceutical Aspects of [^{68}Ga]Ga-PSMA-HBED-CC: A New PET Tracer for Imaging of Prostate Cancer. Pharmaceuticals (Basel). 2014 Jun 30;7(7):779–96.

11. Eder M, Schäfer M, Bauder-Wüst U, Hull W-E, Wängler C, Mier W, et al. ^{68}Ga-complex lipophilicity and the targeting property of a urea-based PSMA inhibitor for PET imaging. Bioconjug Chem. 2012 Apr 18;23(4):688–97.
12. Edlind MP, Hsieh AC. PI3K-AKT-mTOR signaling in prostate cancer progression and androgen deprivation therapy resistance. Asian J Androl. 2014;16(3):378–86.
13. Eisenwiener K-P, Prata MIM, Buschmann I, Zhang H-W, Santos AC, Wenger S, et al. NODAGATOC, a new chelator-coupled somatostatin analogue labeled with [$^{67/68}$Ga] and [^{111}In] for SPECT, PET, and targeted therapeutic applications of somatostatin receptor (hsst2) expressing tumors. Bioconjug Chem. 2002 Jun;13(3):530–41.
14. Fassbender TF, Schiller F, Mix M, Maecke HR, Kiefer S, Drendel V, et al. Accuracy of [^{68}Ga]Ga-RM2-PET/CT for diagnosis of primary prostate cancer compared to histopathology. Nucl Med Biol. 2019;70:32–8.
15. Gibril F, Reynolds JC, Doppman JL, Chen CC, Venzon DJ, Termanini B, et al. Somatostatin receptor scintigraphy: its sensitivity compared with that of other imaging methods in detecting primary and metastatic gastrinomas. A prospective study. Ann Intern Med. 1996 Jul;125(1)(1):26–34.
16. Ginj M, Zhang H, Waser B, Cescato R, Wild D, Wang X, et al. Radiolabeled somatostatin receptor antagonists are preferable to agonists for in vivo peptide receptor targeting of tumors. Proc Natl Acad Sci USA. 2006 Oct;31(44):16436–41. 103(.
17. Gnesin S, Cicone F, Mitsakis P, Van der Gucht A, Baechler S, Miralbell R, et al. First in-human radiation dosimetry of the gastrin-releasing peptide (GRP) receptor antagonist ^{68}Ga-NODAGA-MJ9. EJNMMI Res. 2018 Dec;12(1):108. 8(.
18. Gomez-Pinillos A, Ferrari AC. mTOR signaling pathway and mTOR inhibitors in cancer therapy. Hematol Oncol Clin North Am. 2012 Jun;26(3):483–505. vii.
19. Gourni E, Mansi R, Jamous M, Waser B, Smerling C, Burian A, et al. N-terminal modifications improve the receptor affinity and pharmacokinetics of radiolabeled peptidic gastrin-releasing peptide receptor antagonists: examples of ^{68}Ga- and ^{64}Cu-labeled peptides for PET imaging. J Nucl Med. 2014 Oct;55(10):1719–25.
20. Hofer C, Laubenbacher C, Block T, Breul J, Hartung R, Schwaiger M. Fluorine-18-Fluorodeoxyglucose Positron Emission Tomography Is Useless for the Detection of Local Recurrence after Radical Prostatectomy. EUR. 1999;36(1):31–5.
21. Kähkönen E, Jambor I, Kemppainen J, Lehtiö K, Grönroos TJ, Kuisma A, et al. In vivo imaging of prostate cancer using [68Ga]-labeled bombesin analog BAY86-7548. Clin Cancer Res. 2013 Oct 1;19(19):5434–43.
22. Kelloff GJ, Choyke P, Coffey DS. Challenges in Clinical Prostate Cancer: Role of Imaging. AJR Am J Roentgenol. 2009 Jun;192(6):1455–70.
23. Konings IRHM, Verweij J, Wiemer EC, Sleijfer S. The applicability of mTOR inhibition in solid tumors. Curr Cancer Drug Targets. 2009 May;9(3):439–50.

24. Kumar S, Mohan A, Guleria R. Biomarkers in cancer screening, research and detection: present and future: a review. Biomarkers. 2006 Oct;11(5):385–405.
25. Kurth J, Krause BJ, Schwarzenböck SM, Bergner C, Hakenberg OW, Heuschkel M. First-in-human dosimetry of gastrin-releasing peptide receptor antagonist [^{177}Lu]Lu-RM2: a radiopharmaceutical for the treatment of metastatic castration-resistant prostate cancer. Eur J Nucl Med Mol Imaging. 2019 Sep 3.
26. Liu IJ, Zafar MB, Lai Y-H, Segall GM, Terris MK. Fluorodeoxyglucose positron emission tomography studies in diagnosis and staging of clinically organ-confined prostate cancer. Urology. 2001 Jan 1;57(1):108–11.
27. Maina T, Bergsma H, Kulkarni HR, Mueller D, Charalambidis D, Krenning EP, et al. Preclinical and first clinical experience with the gastrin-releasing peptide receptor-antagonist [^{68}Ga]SB3 and PET/CT. Eur J Nucl Med Mol Imaging. 2016 May;43(5):964–73.
28. Mansi R, Minamimoto R, Mäcke H, Iagaru AH. Bombesin-Targeted PET of Prostate Cancer. J Nucl Med. 2016 Oct;57(Suppl 3):67S–72S.
29. Mansi R, Wang X, Forrer F, Waser B, Cescato R, Graham K, et al. Development of a potent DOTA-conjugated bombesin antagonist for targeting GRPr-positive tumours. Eur J Nucl Med Mol Imaging. 2011 Jan;38(1):97–107.
30. Minamimoto R, Hancock S, Schneider B, Chin FT, Jamali M, Loening A, et al. Pilot Comparison of ^{68}Ga-RM2 PET and ^{68}Ga-PSMA-11 PET in Patients with Biochemically Recurrent Prostate Cancer. J Nucl Med. 2016 Apr;57(4):557–62.
31. Minamimoto R, Sonni I, Hancock S, Vasanawala S, Loening A, Gambhir SS, et al. Prospective Evaluation of ^{68}Ga-RM2 PET/MRI in Patients with Biochemical Recurrence of Prostate Cancer and Negative Findings on Conventional Imaging. J Nucl Med. 2018;59(5):803–8.
32. Nock BA, Kaloudi A, Lymperis E, Giarika A, Kulkarni HR, Klette I, et al. Theranostic Perspectives in Prostate Cancer with the Gastrin-Releasing Peptide Receptor Antagonist NeoBOMB1: Preclinical and First Clinical Results. J Nucl Med. 2017 Jan;58(1):75–80.
33. Pfister J, Summer D, Rangger C, Petrik M, von Guggenberg E, Minazzi P, et al. Influence of a novel, versatile bifunctional chelator on theranostic properties of a minigastrin analogue. EJNMMI Res [Internet]. 2015 Dec 15 [cited 2020 Apr 21];5. Available from: https://www.ncbi.nlm.nih.gov/pmc/articles/PMC4679714/.
34. Price EW, Orvig C. Matching chelators to radiometals for radiopharmaceuticals. Chem Soc Rev. 2014 Jan 7;43(1):260–90.
35. Reubi JC. Peptide receptors as molecular targets for cancer diagnosis and therapy. Endocr Rev. 2003 Aug;24(4):389–427.
36. Reubi JC. Old and new peptide receptor targets in cancer: future directions. Recent Results Cancer Res. 2013;194:567–76.

37. Roivainen A, Kähkönen E, Luoto P, Borkowski S, Hofmann B, Jambor I, et al. Plasma pharmacokinetics, whole-body distribution, metabolism, and radiation dosimetry of ^{68}Ga bombesin antagonist BAY 86-7548 in healthy men. J Nucl Med. 2013 Jun;54(6):867–72.
38. Sah B-R, Burger IA, Schibli R, Friebe M, Dinkelborg L, Graham K, et al. Dosimetry and first clinical evaluation of the new ^{18}F-radiolabeled bombesin analogue BAY 864367 in patients with prostate cancer. J Nucl Med. 2015 Mar;56(3):372–8.
39. Scher HI, Morris MJ, Larson S, Heller G. Validation and clinical utility of prostate cancer biomarkers. Nat Rev Clin Oncol. 2013 Apr;10(4):225–34.
40. Schollhammer R, De Clermont Gallerande H, Yacoub M, Quintyn Ranty M-L, Barthe N, Vimont D, et al. Comparison of the radiolabeled PSMA-inhibitor ^{111}In-PSMA-617 and the radiolabeled GRP-R antagonist ^{111}In-RM2 in primary prostate cancer samples. EJNMMI Res. 2019 Jun 3;9(1):52.
41. Schrecengost R, Knudsen KE. Molecular pathogenesis and progression of prostate cancer. Semin Oncol. 2013 Jun;40(3):244–58.
42. Sinnes J-P, Nagel J, Rösch F. AAZTA5/AAZTA5-TOC: synthesis and radiochemical evaluation with ^{68}Ga, ^{44}Sc and ^{177}Lu. EJNMMI Radiopharm Chem. 2019a Aug 1;4(1):18.
43. Sinnes J-P, Nagel J, Waldron BP, Maina T, Nock BA, Bergmann RK, et al. Instant kit preparation of ^{68}Ga-radiopharmaceuticals via the hybrid chelator DATA: clinical translation of [^{68}Ga]Ga-DATA-TOC. EJNMMI Res. 2019b May 23;9(1):48.
44. Stoykow C, Erbes T, Maecke HR, Bulla S, Bartholomä M, Mayer S, et al. Gastrin-releasing Peptide Receptor Imaging in Breast Cancer Using the Receptor Antagonist ^{68}Ga-RM2 And PET. Theranostics. 2016;6(10):1641–50.
45. Strauss LG, Koczan D, Seiz M, Tuettenberg J, Schmieder K, Pan L, et al. Correlation of the Ga-68-bombesin analog Ga-68-BZH3 with receptors expression in gliomas as measured by quantitative dynamic positron emission tomography (dPET) and gene arrays. Mol Imaging Biol. 2012 Jun;14(3):376–83.
46. Touijer KA, Michaud L, Alvarez HAV, Gopalan A, Kossatz S, Gonen M, et al. Prospective Study of the Radiolabeled GRPR Antagonist BAY86-7548 for Positron Emission Tomography/Computed Tomography Imaging of Newly Diagnosed Prostate Cancer. Eur Urol Oncol. 2019 Mar;2(2):166–73.
47. Tsionou MI, Knapp CE, Foley CA, Munteanu CR, Cakebread A, Imberti C, et al. Comparison of macrocyclic and acyclic chelators for gallium-68 radiolabelling. RSC Adv. 2017 Oct 24;7(78):49586–99.
48. Van de Wiele C, Dumont F, Dierckx RA, Peers SH, Thornback JR, Slegers G, et al. Biodistribution and dosimetry of ^{99m}Tc-RP527, a gastrin-releasing peptide (GRP) agonist for the visualization of GRP receptor-expressing malignancies. J Nucl Med. 2001 Nov;42(11):1722–7.
49. Waldron BP, Parker D, Burchardt C, Yufit DS, Zimny M, Roesch F. Structure and stability of hexadentate complexes of ligands based on AAZTA for efficient PET labelling with gallium-68. Chem Commun (Camb). 2013 Jan 21;49(6):579–81.

50. Wieser G, Mansi R, Grosu AL, Schultze-Seemann W, Dumont-Walter RA, Meyer PT, et al. Positron emission tomography (PET) imaging of prostate cancer with a gastrin releasing peptide receptor antagonist–from mice to men. Theranostics. 2014;4(4):412–9.
51. Yu Z, Ananias HJK, Carlucci G, Hoving HD, Helfrich W, Dierckx RAJO, et al. An update of radiolabeled bombesin analogs for gastrin-releasing peptide receptor targeting. Curr Pharm Des. 2013;19(18):3329–41.
52. Zang J, Mao F, Wang H, Zhang J, Liu Q, Peng L, et al. ^{68}Ga-NOTA-RM26 PET/CT in the Evaluation of Breast Cancer: A Pilot Prospective Study. Clin Nucl Med. 2018 Sep;43(9):663–9.
53. Zhang J, Niu G, Fan X, Lang L, Hou G, Chen L, et al. PET Using a GRPR Antagonist ^{68}Ga-RM26 in Healthy Volunteers and Prostate Cancer Patients. J Nucl Med. 2018;59(6):922–8.

Figures

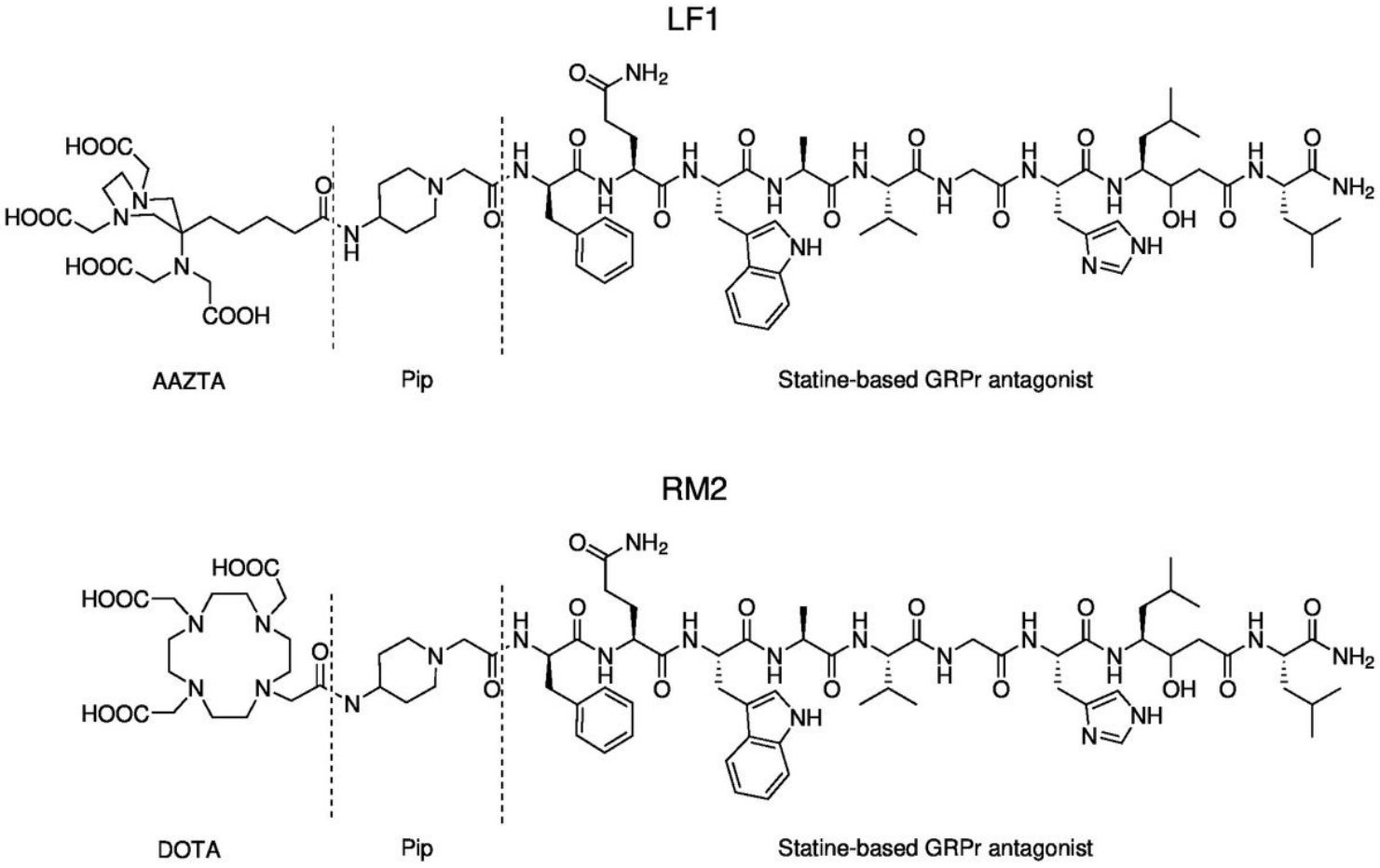

AAZTA: 6-[Bis(carboxymethyl)amino]-1,4-bis(carboxymethyl)-6-methyl-1,4-diazepane

DOTA: 1,4,7,10-tetraazacyclododecane-1,4,7,10-tetraacetic acid

Pip: 4-amino-1-carboxymethyl-piperidine

Figure 1

Schematic structures of LF1 and RM2.

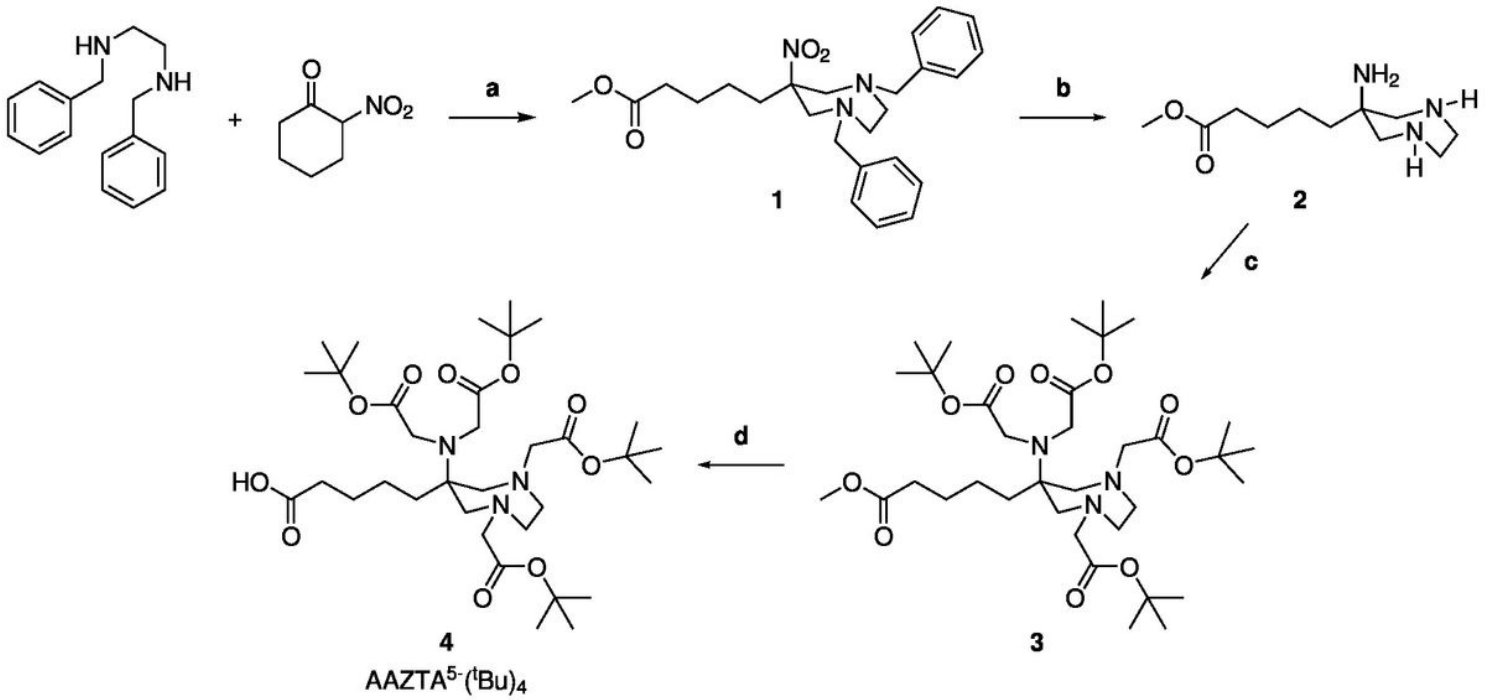

Figure 2

Synthetic scheme of AAZTA5-(tBu)4: (a) paraformaldehyde, MeOH, Amberlyst A21; (b) Pd(OH)2/C, CH3COOH, EtOH, K2CO3; (c) tert-butylbromacetate, MeCN, K2CO3, KI; (d) 1 M LiOH, 1,4-dioxane/H2O (2:1).

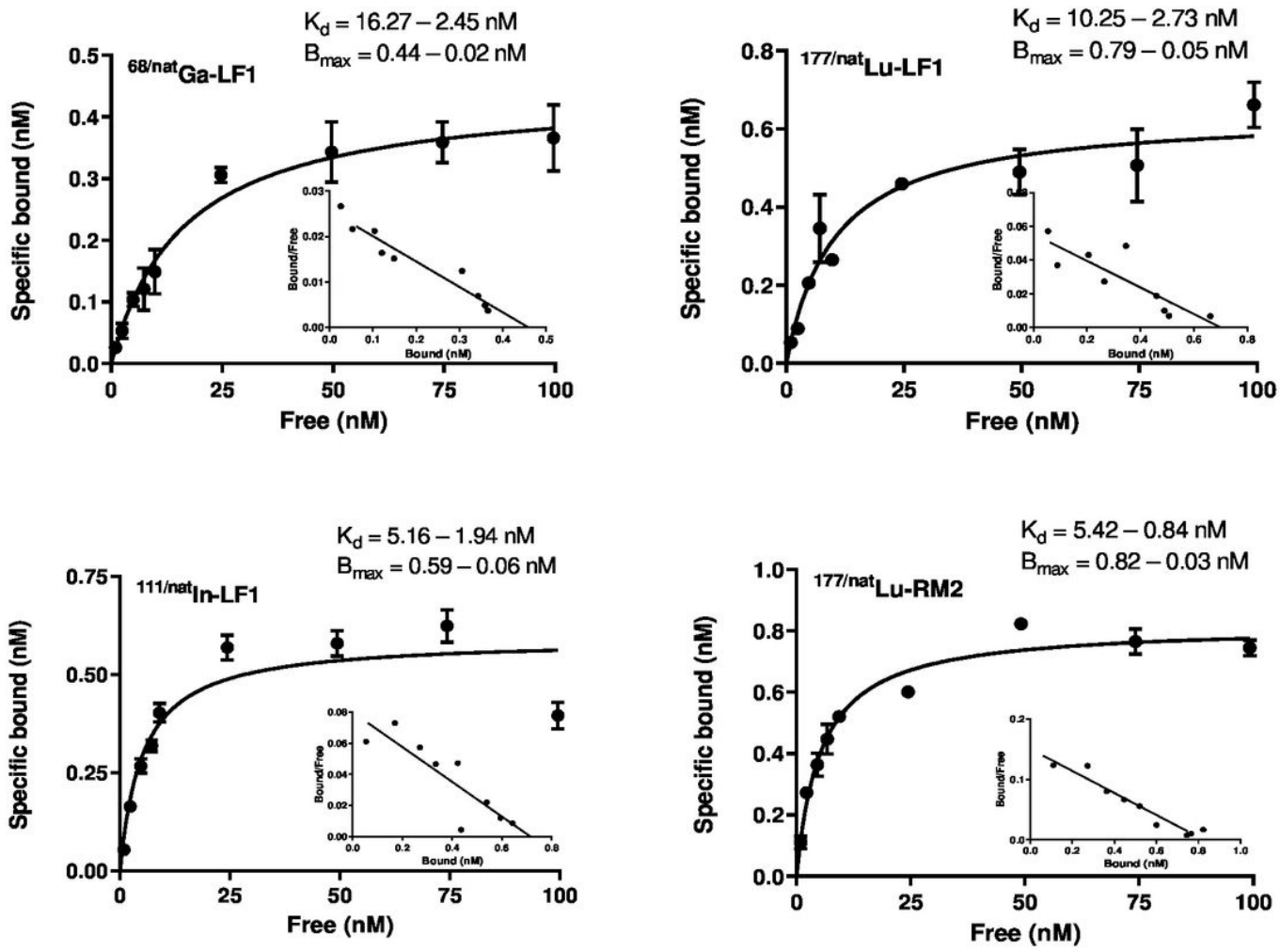

Figure 3

Saturation binding study on intact PC3 cells, using increasing concentrations of 68/natGa-LF1, 177/natLu-LF1, 111/natLF-LF1 and 177/natLu-RM2, ranging from 0.1 to 1,000 nM. Dissociation constant (Kd) and maximum number of binding sites (Bmax) were calculated from nonlinear regression analysis using GraphPad Prism.

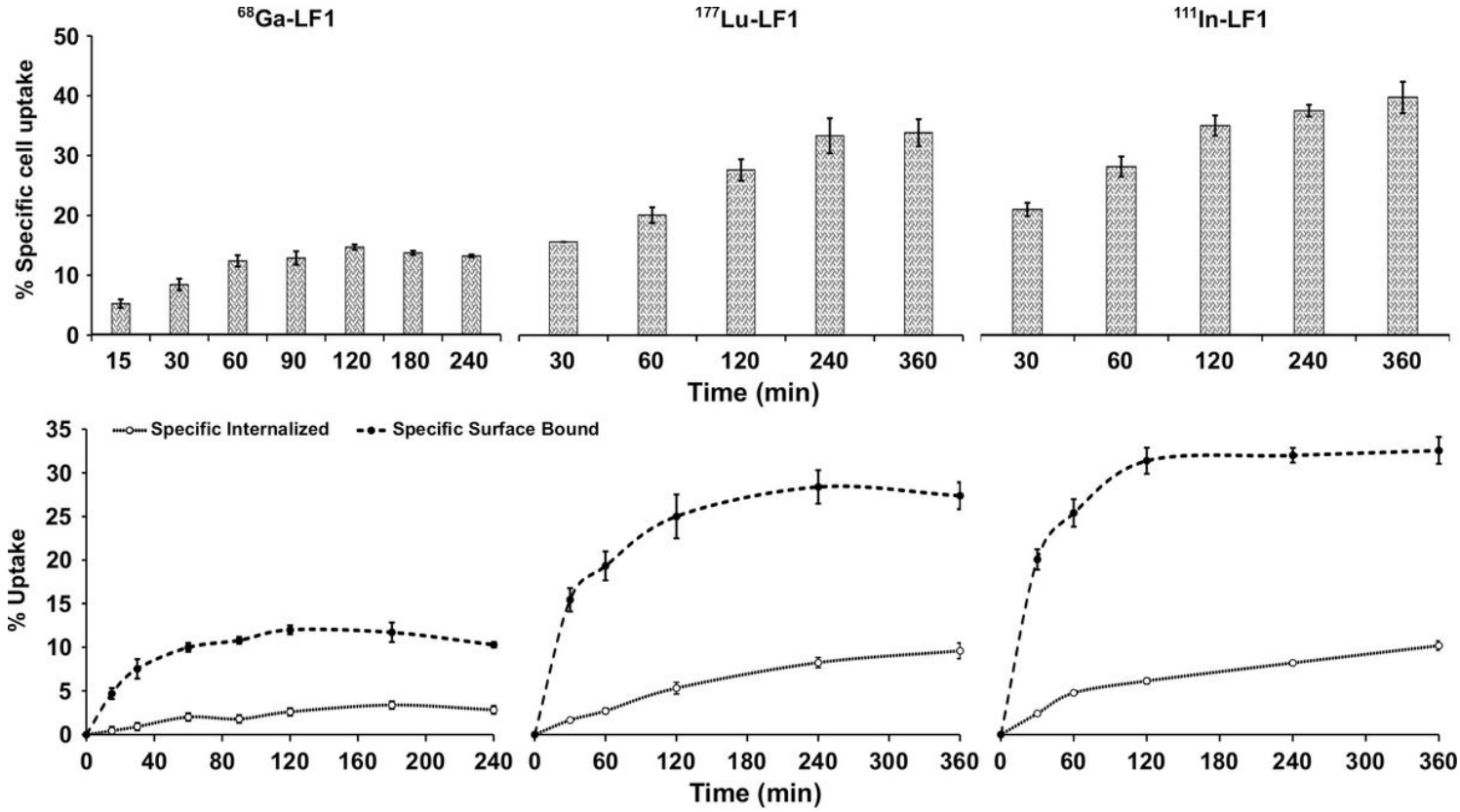

Figure 4

Specific cell uptake, internalization rate specific surface uptake after the incubation of PC3 cells with 68Ga-LF1, 177Lu-LF1, 111In-LF1 within 4 or 6 h at 37°C. A-C: Cell uptake calculated as cell surface-bound and internalized fraction. D-F: Receptor-specific internalization and specific surface bound activity expressed as percentage of the applied radioactivity. Nonspecific binding was determined in the presence of 1 μM Tyr4-BN.

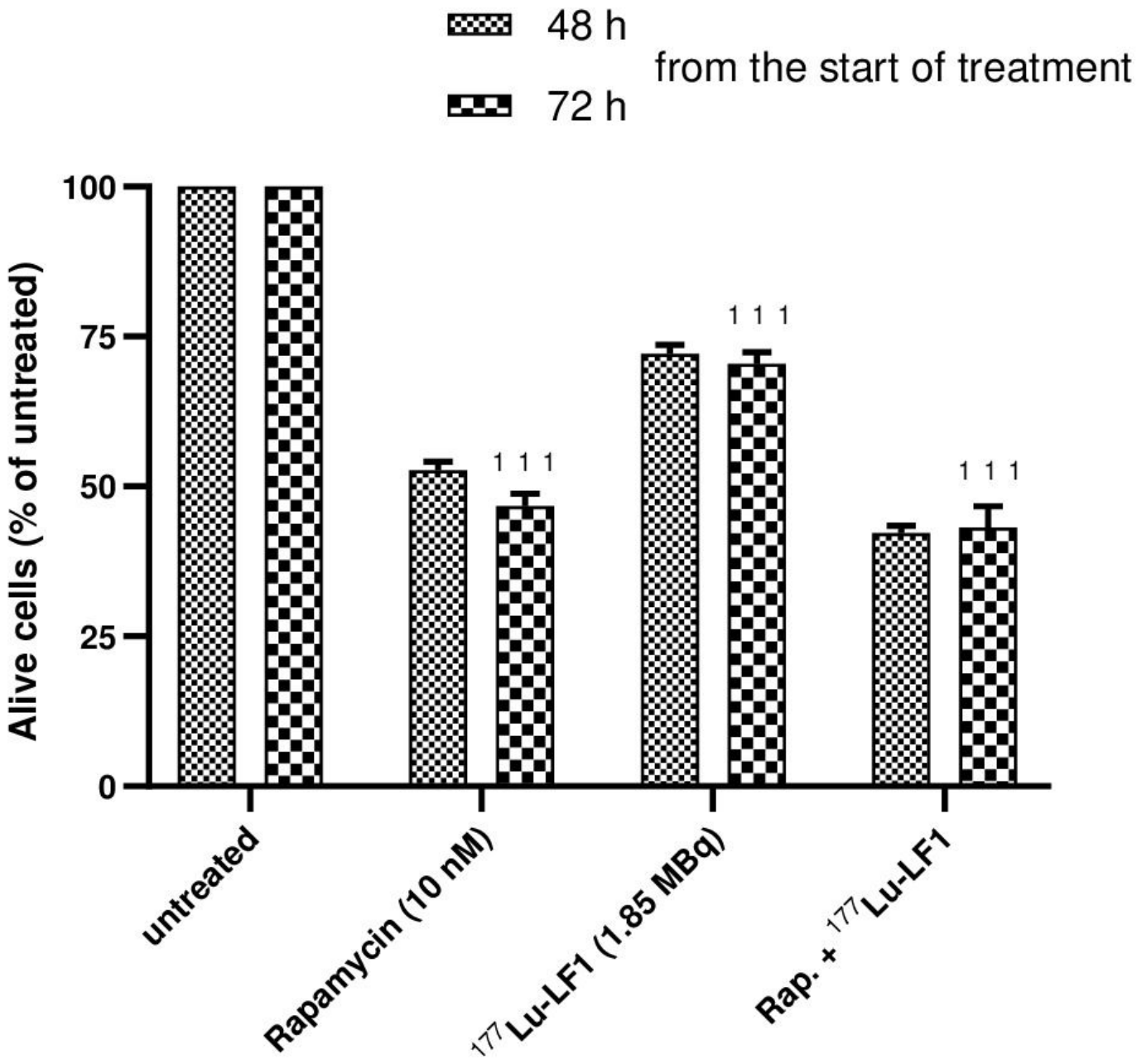

Figure 5

In vitro therapy assessing the effect of monotherapy (rapamycin or 177Lu-LF1) and combination therapy (rapamycin and 177Lu-LF1) on PC3 cells.